Packing fractions and maximum angles of stability of granular materials

J. Olson, M. Priester, J. Luo, S. Chopra, and R. J. Zieve
Physics Department, University of California, Davis, California 95616
(Received 17 December 2004; published 16 September 2005)

In two-dimensional rotating drum experiments, we find two separate influences of the packing fraction of a granular heap on its stability. For a fixed grain shape, the stability increases with packing fraction. However, in determining the relative stability of different grain shapes, those with the *lowest* average packing fractions tend to form the most stable heaps. We also show that only the configuration close to the surface of the pile figures prominently.

DOI: 10.1103/PhysRevE.72.031302 PACS number(s): 45.70.Ht, 45.70.Cc

I. INTRODUCTION

Granular materials are studied in materials science, geology, physics, and engineering [1]. Their unusual dynamical behavior has attracted much recent attention [2–4], and even the more staid static issues generate steady interest [5,6]. One question is how much of granular behavior can be derived from purely geometrical considerations. In practical materials, particle deformation and surface effects such as cohesion and agglomeration also play major roles, masking the influence of geometry. Furthermore, studying grain shape is a difficult endeavor. The experimental challenge is in creating uniform but nonspherical shapes. Recent efforts include two-dimensional studies of regular pentagons [7,8] and a three-dimensional experiment using M&M's [9]. On the theoretical side, the problem is how to treat the interaction of grains as they move past each other.

Work linking geometry to behaviors other than packing is yet more scarce. One rare attempt involves predicting avalanches in a granular pile [10], a question at the border between statics and dynamics. Granular piles, such as sandpiles, exhibit characteristic angles for their free surfaces. One is the repose angle, below which the pile is stable. If the surface becomes steeper than the repose angle—for example, if the pile is tilted or if new grains are added—then the heap may undergo an avalanche in which grains all along the slope move, resulting in a lower angle. In practice, avalanches do not begin until the angle exceeds what is known as the maximum angle of stability, which is typically several degrees larger than the repose angle. Once started, an avalanche continues until the pile surface is again less steep than the repose angle. Albert *et al.* [10] derive a maximum angle of stability from local geometry, beginning with a regular tetrahedron of spheres. In addition to safety issues, understanding avalanches is important in fields such as geology and soil mechanics, where granular matter can flow along inclined surfaces.

Both theoretical and experimental work relate the packing fraction of a heap to its stability, for the special case of spherical grains [11–13]. The experiments involve packing spheres under pressure to achieve different initial packing fractions, then tilting the heap and noting the angle of the first avalanche. As the spheres are packed more tightly, the maximum angle of stability increases. In both these measurements, the packing fraction is known only for the initial, artificially constructed arrangement. They do not test whether the packing fraction also affects stability in the configurations that actually occur after an avalanche. One set of these experiments [11] uses not only smooth spheres but also "rough" spheres and angular grains. The two very different nonspherical shapes sustain similar maximum angles, higher than that of smooth spheres.

Here we revisit the role of density, extending our study to configurations that occur naturally as a result of prior avalanches and to nonspherical grains. We work in two dimensions, which makes visualizing an entire configuration much easier than for a three-dimensional heap. Our grains are composed of spherical ball bearings, welded together in clusters of up to nine balls. The balls in each cluster are part of a two-dimensional triangular lattice. Working with sphere clusters has various advantages. The maximum possible density is always that of a triangular lattice of the component spheres. Spheres minimize friction and blocking effects as the shapes move past each other. Finally, our system lends itself to comparison with computer experiments, since checking for overlaps, a challenging part of typical simulations, is trivial for sphere clusters.

We find that the packing fraction indicates pile stability for both spherical and nonspherical shapes, but with a twist. When comparing piles composed of different grains, *low* average packing fraction indicates stability. After presenting our experimental results, we offer an explanation for this behavior and other observations about the influence of grain shape.

II. PROCEDURE

As described elsewhere [14], we weld together $\frac{1}{8}$-in.-diameter carbon steel ball bearings to make dimers; trimers (three balls in a straight line); triangles of three or six balls; diamonds of four, six, or nine balls; trapezoids of five or seven balls; and hexagons of seven balls. The left column of Table I illustrates these shapes.

Our tumbler, shown schematically in Fig. 1, is a sheet of aluminum, $\frac{1}{8}$-in.-thick with a circular hole 14 in. in diameter cut from its center. The aluminum is sandwiched between two $\frac{1}{2}$-in.-thick sheets of Plexiglas, which constrain the balls to move in a single layer. The plane of the tumbler is vertical. A central axle attaches the tumbler to a stepper motor which

TABLE I. Average maximum angle of stability (θ_m), repose angle (θ_r), and average packing fraction immediately before an avalanche (ρ_i) for 11 shapes in a container with irregular boundary. Standard errors are also given. Shapes are ordered by increasing θ_m.

	θ_m	$\sigma(\theta_m)$	θ_r	$\sigma(\theta_r)$	ρ_i
•	33.8	0.7	26.3	0.6	0.8204
⁂	39.5	0.4	29.3	0.5	0.7764
⁂	41.2	0.5	31.3	0.3	0.8058
••	42.0	0.6	32.9	0.5	0.8238
•••	43.8	1.0	34.5	0.8	0.7974
⁂	44.9	0.8	33.6	0.7	0.7718
⁂	48.7	1.3	35.0	1.0	0.7097
⁂	49.1	1.0	38.2	0.9	0.7696
••••	50.6	1.1	38.7	0.7	0.7609
⁂	50.9	1.5	36.6	0.9	0.7627
⁂	51.8	1.0	37.8	0.9	0.7573

controls the rotation rate. For all measurements here the rotation rate is about 500 μHz, or one full turn in about 30 min. We use this slow speed so that the rotation of the container itself during an avalanche remains negligible, and the avalanches are discrete events. To prevent the balls from sliding along the wall of the container during rotation, a thin strip of rubber is glued to the inner edge of the aluminum. In some measurements, as described below, an irregular boundary was created by attaching aluminum triangles along the edge of the hole.

For each shape we use a total mass of 365.6±0.3 g, so that the grains fill a similar portion of the tumbler. Since the grains are initially dropped individually onto a growing heap, the resulting configurations may differ from those reached after avalanches in the tumbler. In this work we investigate

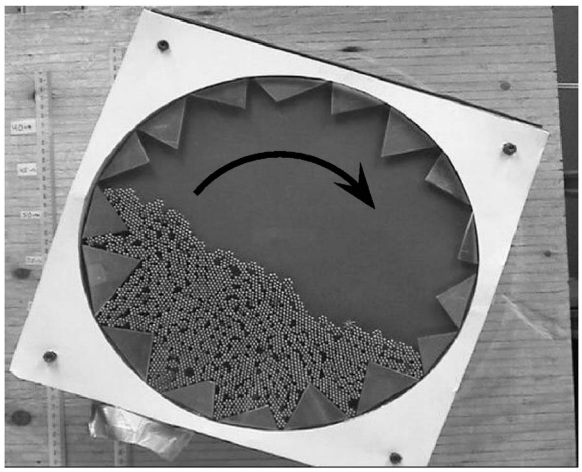

FIG. 1. Tumbler with two-dimensional heap of hexagonal grains, just after an avalanche. Rotation is clockwise within the plane of the container. The triangles transform the container boundary from a circle to an irregular shape.

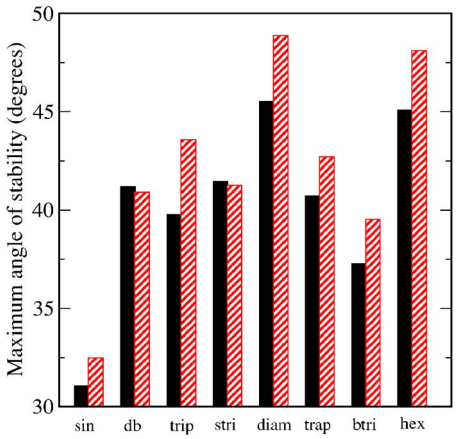

FIG. 2. (Color online) Average angle for avalanche onset for eight different shapes. Solid (black): container with circular boundary. Striped (red): container with irregular boundary. The shapes used are indicated along the horizontal axis, arranged in order of size.

the class of configurations that can be obtained by successive avalanches. Hence, to eliminate the effects of the grain loading, we rotate the tumbler for at least 30 min *before* making any measurements. We then rotate the tumbler for an additional 30 min, which generally yields 20–30 discrete avalanches and record this rotation with a digital video camera. Afterwards the avalanches are identified by eye, and the video frames immediately before and after each avalanche are uploaded to a computer.

To simplify the image processing, we use a solid red background inside the tumbler and solid white around the outside. These colors allow a computer program to identify easily the region occupied by the heap. Since we know both the total mass of the grains and the mass per grain, we can convert the area of the heap to a packing fraction. We also fit a line to the free surface of the heap and use it to define the angle from horizontal of the surface. In this way we extract the angle and packing fraction for each image.

On removing the shapes from the tumbler after a measurement, we sort and count any broken grains. The maximum angle of stability is sensitive to broken shapes; so if over 10% of the original pieces break during a measurement, we discard the data and run that shape again. In most cases breakage is less than 3% of the original shapes. Concern about broken pieces figures in our 30-min observation time. Although most of the breakage occurs upon loading the shapes into the tumbler, we cannot assess it until after collecting all the data and removing the grains. With a longer data collection time the breakage does increase slightly. More importantly, we run the risk of having to discard more data if we do find many broken pieces.

III. RESULTS AND DISCUSSION

The solid bars of Fig. 2 show the average angle just before an avalanche for several different shapes. Standard errors are typically 1° and never more than 1.5°, so the variations among shapes are significant. Two shapes, diamonds

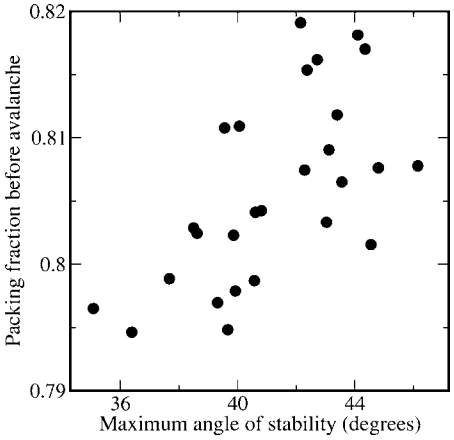

FIG. 3. Packing fraction and critical angle for the individual avalanches of the small triangle shapes (three balls). The correlation coefficient is 0.626.

and hexagons, form significantly more stable heaps than the other shapes.

These angles are very different from the results of our previous work in a rectangular container, which allows a single-crystalline region [15]. To test that boundary effects do not dominate the variations we find among shapes, we inserted 16 triangles in an irregular pattern along the surface of the circle and repeated the measurements. The results, shown as striped bars in Fig. 2, are qualitatively the same. Diamonds and hexagons remain much more stable than the other shapes.

The quantitative differences between the containers could be an effect of the boundary surface. Another contribution may come from small differences in the numbers of broken shapes in the two sets of measurements.

In the irregular container, we extended the measurements to several additional shapes. All data from this setup are shown in Table I. There is no clear pattern of how geometry affects critical angle, beyond the general observation that larger shapes support higher angles. Given the scalloped boundaries of our shapes, which allow some interlocking, this seems natural.

We also characterize each configuration by its packing fraction. Figure 3 shows the packing fraction and maximum angle attained for each avalanche with the small triangles. As in the earlier work with compacted media in three dimensions [11,12,18], the two properties are positively correlated. This also agrees with the observation that interlocking and jamming, which can increase the stability angle, occur more easily at higher packing fractions [15]. Strikingly, eight of the ten other shapes exhibit a similar correlation between the packing fraction and the angle of the ensuing avalanche, with correlation coefficients between 0.4 and 0.71. (The remaining shapes, the large triangles and large trapezoids, show no significant correlation between the two.) Thus we confirm experimentally that a connection between the pile density and maximum angle of stability exists for a variety of shapes, although it appears not to be universal.

Even more importantly, our measurements relate these properties for naturally occurring configurations—those that result from previous avalanches—rather than merely for artificially compacted initial arrangements. In this experiment, we do not actively control the packing fraction, but simply measure its value in each configuration. Thus the range of packing fractions in Fig. 3 arises solely from statistical variation among arrangements of nominally identical preparation procedures and is much smaller than for earlier work on compressed piles. That we nonetheless detect an influence of pile density on stability highlights its importance. The similarity between our results and those on deliberately compacted systems, and in both two and three dimensions, enhances the extent of a quite general relationship between packing fraction and stability. Furthermore, in many practical situations, grain arrangement is in fact determined from previous avalanches.

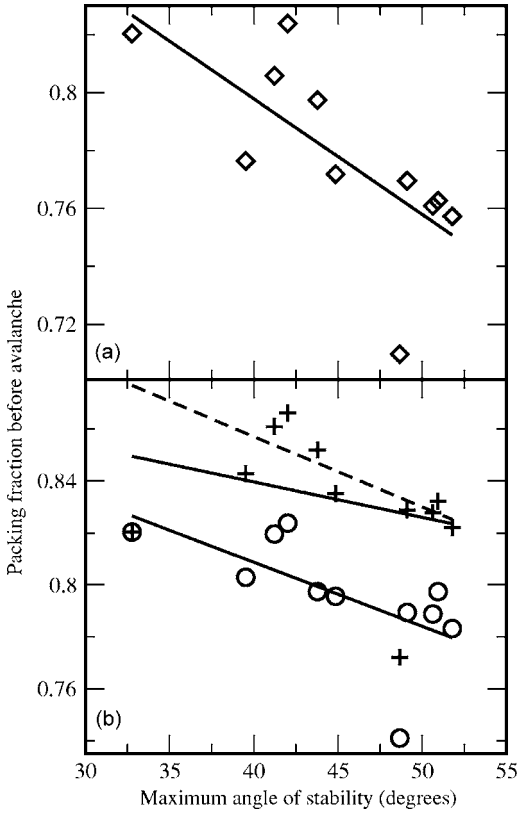

FIG. 4. (a) Average packing fraction and maximum angle of stability for the 11 different shapes. Each diamond represents one shape. Since the θ_m values of Table I are the same angles shown here, the shape corresponding to each data point can be read from the table. The line is simply a linear fit used as a guide to the eye. (b) Different definitions of packing fraction for the agglomerates also show the negative correlation with stability; see text.

In addition to connecting pile density and stability angle for the individual avalanches of each shape, we compare the behavior among shapes. Here a far less intuitive influence of packing fraction appears. Figure 4(a) again plots packing fraction against maximum angle, but here each point represents an average over all avalanches for a single shape. Now the correlation is actually in the *opposite* direction from that of Fig. 3: high packing fractions tend to yield *low* critical angles. The identity of the points can be seen in Table I, since θ_m in the table is exactly the angle shown in the graph.

Note that the standard errors in the angles, as listed in the table, are of the order of 1°. This is significantly smaller than the variation among shapes, which covers more than 15°. We confirmed that the given standard errors are reliable by repeating the procedure on several of the shapes: loading them into the tumbler afresh and recording a new set of avalanches. In each case the standard deviations for the two trials were comparable. The average angle always differed by less than twice the standard error and in all but one case by less than 1.5 times the standard error. Arriving at the repeatable procedure we now use took some care; in fact, the nonreproducibility of some preliminary trials alerted us to the large effect of broken clusters.

Assessing the uncertainty in the packing fractions is more complicated. The maximum stability angles of successive avalanches show no correlation, but the packing fractions do. No correlation in packing fraction remains after six avalanches though, giving typical standard errors around 0.005. As for the stability angles, we confirmed the validity of the standard errors by the repeated runs on several shapes. The range of packing fractions is over 0.06, even without considering the extremely low packing fraction of the hexagons, so again the measured variations are statistically significant. The data of Fig. 4 would change little if we averaged larger numbers of avalanches.

The apparently opposite influence of packing fraction within a shape and across different shapes may be understood by considering how the pile is formed. From our measurements on individual shapes, we know that tightly packed configurations are more stable. During an avalanche, a necessary condition for flow to cease is a stable instantaneous arrangement of grains. Furthermore, grain motion always requires expansion so that the particles have room to move [16]. As an avalanche stops, the packing fraction again increases. Thus the moving grains pass through configurations with a range of packing fractions. Many of the arrangements with the lowest packing fractions are unstable or, at least, not stable enough to absorb the momentum of the moving grains. As the packing fraction increases, the arrangements are more likely to be stable and allow the avalanche to stop. If a shape has a low average packing fraction, its avalanches must stop relatively early, and the shape is likely to support a wide range of stable configurations.

Rotation is another means of sampling different grain arrangements, since the stability of any configuration depends on the direction of gravity. If a particular grain shape allows more stable arrangements than usual, then the new configurations reached by tilting a heap of such grains are more likely to be stable. On average the heap will take longer to reach an unstable configuration and trigger an avalanche. The negative correlation we observe between packing fraction and maximum angle of stability comes about because low-density configurations are most likely to occur with shapes of generally high stability. This logic implies that particularly high critical angles should be found for tightly packed grains with a low random loose packing value.

One might wonder whether the observed trend could be an artifact of our treatment of packing fraction. Figure 5 shows three possibilities for the effective area of a three-ball triangle. The actual cross section of the balls [case (a)] could be augmented by the enclosed empty space [case (b)] or even by the external space that other grains cannot reach because of the scalloped edge [case (c)]. The theoretical maximum packing fraction is 1 for case (c), making it the largest plausible effective area. For case (a), all our shapes have the same theoretical maximum packing fraction of $\pi/2\sqrt{3}$ and achieve this density for significant patches. This can be seen even for the hexagons of Fig. 1, and hexagons have by far the lowest packing fractions of all our shapes. To the extent that the agglomerates form similar arrangements to individual balls, the actual cross section is the best choice of area, since the internal space would be forbidden even for single balls. However, the larger agglomerates do support holes in their configurations comparable in size to their outer dimensions. If the packings were completely dominated by such holes, then the small gaps between individual spheres would become irrelevant and it would be natural to use case (b) or even case (c) as the effective filled area. In Fig. 4(b) we show that redefining the effective packing fraction using cases (b) (circles) or (c) (crosses) does not eliminate the connection to pile stability. The solid lines are again linear fits. The dashed line is a linear fit to the crosses that omits the two low-density outliers, single balls and hexagons. The motivation is that treatment (c) places single balls on a different footing from the other shapes, with a much lower theoretical density. We remove the hexagons as well to show that the correlation does not arise solely from the hexagons' unusually low packing fraction.

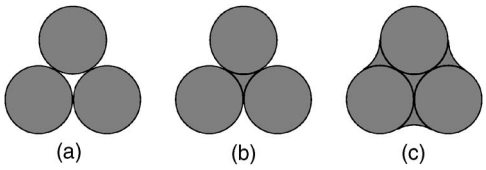

FIG. 5. Three possibilities for the effective area of a three-ball triangle, for evaluating packing fractions. (a) Cross section of balls themselves, used in Fig. 4(a); maximum packing fraction $\pi/2\sqrt{3} \approx 0.907$ for all shapes. (b) Balls plus interior spaces, used for circles in Fig. 4(b); maximum packing fraction $\frac{1}{6}+5\pi/12\sqrt{3}$ for these triangles but varies with shape. (c) Balls, interior spaces, and unfillable outer spaces, used for squares in Fig. 4(b); maximum packing fraction 1 for all shapes except single balls.

Yet another effective area calculation has proven useful for three-dimensional disordered clusters. Fine dry powders near the jamming threshold agglomerate into clusters [17]. The cluster diameter is nearly independent of the individual particle size, so agglomerates of the finest powders contain the most particles. The finest powders also exhibit the lowest packing fraction at jamming. Interestingly, our system has a similar behavior, in that the shapes composed of the most particles also tend to have both low packing fractions and high maximum angles. When the fine powder agglomerates are assigned an effective volume by using the radius of gyration to define an equivalent spherical shell, the resulting effective packing fractions at jamming are independent of particle size [17]. For our system though, with substantial order throughout and perfect order within the clusters, the analogous equivalent hoop calculation makes little sense.

TABLE II. Correlations among packing fractions before (ρ_i) and after (ρ_f) an avalanche, maximum angle of stability (θ_m), angle of repose (θ_r), and change in angle during an avalanche ($\Delta\theta$). Values are the averages of the correlation coefficients calculated for all 11 shapes.

	ρ_i	θ_r	ρ_f	$\Delta\theta$
θ_m	0.475	−0.269	0.032	0.841
ρ_i		−0.105	0.613	0.399
θ_r			0.290	−0.728
ρ_f				−0.138

The effective packing fraction from this treatment has seven times the variation of the original packing fraction of Fig. 4(a) and exceeds 1 for half the clusters, clear signs that the model is inappropriate. Indeed, for the limiting case of long straight clusters in an ordered arrangement, this version of effective packing fraction becomes infinite. The fundamental problem—that a hoop poorly approximates elongated shapes—applies even for our small clusters.

Monitoring successive avalanches allows us to study other correlations among the configurations as well. Table II deals with five variables: packing fraction and angle before and after each avalanche, and the change in angle. The table shows the correlation between each pair of quantities, averaged over all 11 shapes. There is no significant correlation between initial packing fraction and repose angle or between final packing fraction and maximum angle of stability. We also find directly that the angles of successive avalanches are uncorrelated. Previous experiments found a similar lack of correlation in the size of successive avalanches [18], suggesting that a single avalanche completely resets the system memory.

On the other hand, the packing fractions of successive avalanches (or, equivalently, the packing fractions before and after a single avalanche) are highly correlated. This is hardly surprising, given that any single avalanche leaves about half of the ball bearings completely unaffected. In addition to the stationary regions, there are typically several large clumps within the pile that rotate slightly during the avalanche but have no change in their internal arrangements. With this in mind, the correlation is if anything lower than expected. The implication is that the density varies more strongly in the top few layers, which reconfigure completely during an avalanche, than in the rest of the heap.

Combining these observations, we see that significant packing fraction correlations between consecutive avalanches arise from the stationary lower layers, but that successive avalanches show no correlation in stability angle. Consequently, the correlation between packing fraction and maximum angle of stability must depend *only* on the packing fraction in the upper, mobile layers. The heap density within these layers, which we cannot easily calculate, would likely show a much stronger relationship with the stability angle than the overall density as in Fig. 3.

Finally, there is a small but consistent negative correlation between critical angle and repose angle. This may happen because more momentum builds up during an avalanche that begins on a steep slope, enabling the avalanche to continue longer. The one exception is the single balls, which have positive correlation between critical and repose angles as well as much weaker connections between avalanche size and the initial and final angles.

IV. CONCLUSION

We have shown that the packing fraction plays a dual role in predicting the stability of a two-dimensional heap. For a given grain shape, denser packings are generally more stable, and we have extended this result beyond the previous measurements on artificially packed spheres in three dimensions. However, when comparing different shapes, those with the *lowest* packing fractions have the highest maximum stability angles on average. We also find that only the packing fraction of the top layers of the heap figures strongly in the stability, so the correlation would likely be much more pronounced if the packing fraction calculation could be confined to this region. Identifying precisely the portion of a pile in which the packing fraction influences stability is an interesting direction for further work.

We are also expanding our work to heaps containing a mixture of grain shapes, which drastically enlarges the phase space for measurements. In the course of the present work, we observed that a small fraction of broken shapes can significantly change the critical angle. We expect tests of shape mixtures to help explain why.

ACKNOWLEDGMENTS

We thank C. Olson and C. Reichhardt for discussions about the influence of shape on stability. This work was supported by the National Science Foundation under Grant Nos. DMR-9733898 and PHY-0243904.

[1] J. Duran, *Sands, Powders, and Grains: An Introduction to the Physics of Granular Materials* (Springer-Verlag, New York, 2000).
[2] A. Kudrolli, Rep. Prog. Phys. **67**, 209 (2004).
[3] J. Rajchenbach, Adv. Phys. **49**, 229 (2000).
[4] R. P. Behringer, Int. J. Bifurcation Chaos Appl. Sci. Eng. **7**, 963 (1997).
[5] S. F. Edwards and D. V. Grinev, Adv. Phys. **51**, 1669 (2002).
[6] D. Bideau and A. Hansen, *Disorder and Granular Media* (North-Holland, Amsterdam, 1993).
[7] F. Cantelaube, Y. Limon-Duparcmeur, D. Bideau, and G. H. Ristow, J. Phys. I **5**, 581 (1995).
[8] Y. Limon Duparcmeur, A. Gervois, and J. P. Troadec, J. Phys.: Condens. Matter **7**, 3421 (1995).

[9] A. Donev, I. Cisse, D. Sachs, E. A. Variano, F. H. Stillinger, R. Connelly, S. Torquato, and P. M. Chaikin, Science **303**, 990 (2004).
[10] R. Albert, I. Albert, D. Hornbaker, P. Schiffer, and A. L. Barabasi, Phys. Rev. E **56**, R6271 (1997).
[11] R. L. Brown and J. C. Richards, *Principles of Powder Mechanics* (Pergamon, Oxford, 1966).
[12] J. R. L. Allen, Geol. Mijnbouw **49**, 13 (1970).
[13] P. Evesque, D. Fargeix, P. Habib, M. P. Luong, and P. Porion, Phys. Rev. E **47**, 2326 (1993).
[14] I. C. Rankenburg and R. J. Zieve, Phys. Rev. E **63**, 061303 (2001).
[15] C. J. Olson, C. Reichhardt, M. McCloskey, and R. J. Zieve, Europhys. Lett. **57**, 904 (2002).
[16] O. Reynolds, Philos. Mag. **20**, 469 (1885).
[17] J. M. Valverde, M. A. S. Quintanilla, and A. Castellanos, Phys. Rev. Lett. **92**, 258303 (2004).
[18] P. Evesque, Phys. Rev. A **43**, 2720 (1991).